

MICROSTRUCTURAL ANALYSIS OF ASYMMETRIC DILUTION BY ROTATING DIRECT METAL DEPOSITION

In this study, cross-section analysis was performed on a novel rotating direct-metal deposition method capable of preliminary surface treatment and damage repair of cylindrical inner walls. The cross-sectional shape, microstructure, and metallurgical composition were analyzed to verify feasibility. No defects such as porosity or cracks were found in the cross section, but asymmetric dilution was observed because of the non-coaxial powder nozzle. Microstructural coarsening was confirmed over a higher dilution area by high-magnification optical microscope images. As the dilution ratio was increased, hard carbides in the dendrite were bulk-diffused into inter-dendrite spaces, and the toughness was lowered by Fe penetration into the deposit. Therefore, the increased laser heat input can be modulated to the typical dilution by decreasing the laser scanning velocity.

Keywords: Rotating direct metal deposition, Asymmetric dilution, Cross-sectional analysis, Microstructure, Metallurgical composition

1. Introduction

Components with cylindrical bores such as engine blocks, cannon barrels, and plastic extruders are exposed to high-temperature and high-pressure environments for long periods, result in cavitation, cracking, and delamination on the inner wall. Frequent replacements cause enormous financial and material losses because of manufacturing process and their high material usage. In recent years, a technique of remanufacturing to the same level as a new product has been applied to overcome this disadvantage. The damaged part can be repaired by welding, but welding is disadvantageous because of the poor bonding quality under high heat input [1].

In this study, the bonding performance of rotating direct-metal deposition (Fig. 1), a novel technique to repair damaged cylinder inner walls, was evaluated. The direct-metal deposition by laser and powder can be used for preliminary surface treatment or repair to extend the service life of a part. However, unlike planar deposition, the powder is injected to a location above the laser focus because the powder flows down due to gravity. Thus, the upper part of the laser path is more disturbed by the powder, which reduces the heat energy flowing into the base material. The less-disturbed lower part receives larger heat input to the base material, which increases dilution. This phenomenon causes differences in dilution (Fig. 2), which is an index of the bonding performance of the laser deposition.

To analyze this, Co-based Stellite 6 powder was deposited on a pipe inner wall of AISI 4140 Cr-Mo structural alloy steel.

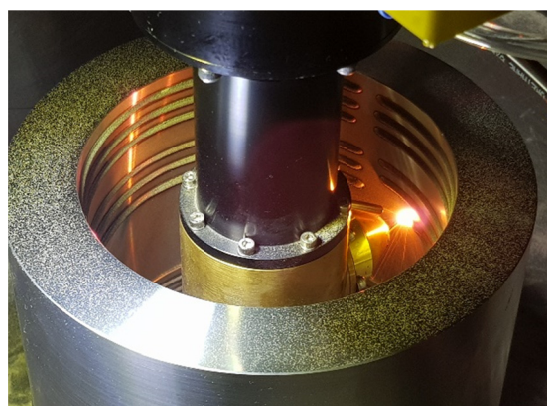


Fig. 1. Rotating direct-metal deposition experiments on cylinder inner wall

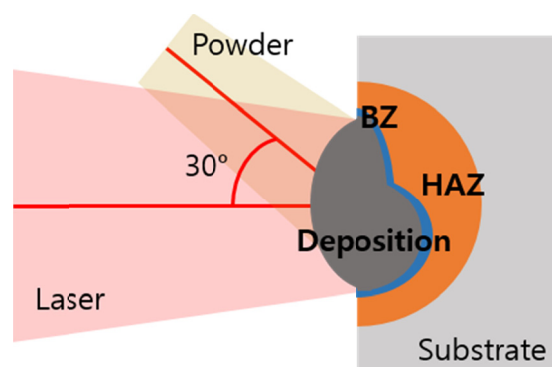


Fig. 2. Asymmetric dilution in non-coaxial rotating direct-metal deposition. BZ: bonding zone; HAZ: heat-affected zone

* AJOU UNIVERSITY, DEPARTMENT OF MECHANICAL ENGINEERING, 206, WORLD CUP-RO, YEONGTONG-GU, SUWON-SI, GYEONGGI 16499, KOREA

** EUROVISION LASER CO., LTD, GUNPO, REPUBLIC OF KOREA

Corresponding author: princaps@ajou.ac.kr

Firstly, the cross-section of asymmetric dilution was investigated under variations in laser power, laser scanning velocity, and powder feed rate. Secondly, the microstructures of typical dilution and asymmetric dilution were analyzed. Thirdly, differences in chemical composition distributions and hard phase formation were analyzed. Finally, the experimental research on rotating direct-metal deposition is reviewed and a method for solving asymmetric dilution is suggested. This study contributes to preliminary surface treatment and damage repair of cylinder inner walls by rotating direct-metal deposition.

2. Experimental

A continuous-wave 970-nm diode laser (Terradiode, 2 kW direct diode laser) was used for deposition experiments. The powder from the feeder (Sulzer Metco, TWIN 10-C) was mixed with nitrogen gas and injected in the laser spot. Coolant at 22°C was supplied to cool the optical elements and parts. Mixed argon and nitrogen gas was sprayed on the deposition area to suppress the oxidizing atmosphere during the process.

Co-based Stellite 6 powder was used for deposition in the AISI 4140 Cr-Mo specimen manufactured in a hollow cylinder shape with the inner diameter of 128 mm, outer diameter of 180 mm, and height of 100 mm. The chemical composition is shown in Table 1. The powder particle size is 50-180 μm and the melting temperature is 1285-1410°C [2].

TABLE 1

The chemical composition of Stellite 6 and substrate (wt. %)

	C	Cr	Si	W	Fe	Co	Ni	Mn	Mo	Others
Stellite 6	1.6	28.7	1.0	3.9	0.4	Bal.	1.6	0.3	0.6	—
AISI 4140	0.43	1.1	0.24	—	Bal.	—	0.22	0.79	0.19	0.198

The experimental conditions were varied by controlling the main deposition process parameters of the laser power, laser scanning velocity, and powder feed rate. Experiments were

conducted at high and low values for each condition based on the laser power of 1.4 kW, laser scanning velocity of 6 mm/s, and powder feed rate of 12 g/min. The experimental conditions are shown in Table 2.

TABLE 2

Processing parameters for rotating direct-metal deposition experiments

	Laser power (kW)	Laser scanning velocity (mm/s)	Powder feed rate (g/min)
(a)	1.4	6	12
(b)	1.6	6	12
(c)	1.4	4	12
(d)	1.4	6	14

In order to minimize heat damage to the cross-section during the cutting process, the wire electric discharge machining (EDM) was used. And the specimens were mounted and polished with sand paper and diamond paste. The cross-sectional shapes and microstructures were analyzed by optical microscopy (BX51M, Olympus) and field-emission scanning electron microscopy (FE-SEM; JSM-6700F, JEOL). Chemical composition was analyzed by energy dispersive X-ray spectroscopy (EDS) equipped in the FE-SEM.

3. Results and discussion

Fig. 3 shows the cross-sectional shape. The mean process condition (a) forms deposits with the relatively small size of 2.50 mm in width and 0.81 mm in height because it has low deposition efficiency. On the other hand, the high-power condition (b) allows deposits of 2.78 mm in width and 1.08 mm in height. Asymmetric dilution, as described in Fig. 2, is confirmed; the microstructure and metallurgical composition are discussed in the next paragraph. The low laser scanning velocity condition (c) forms deposits of 2.55 mm in width and 1.05 mm in height; asymmetric dilution is remarkably reduced. The high powder

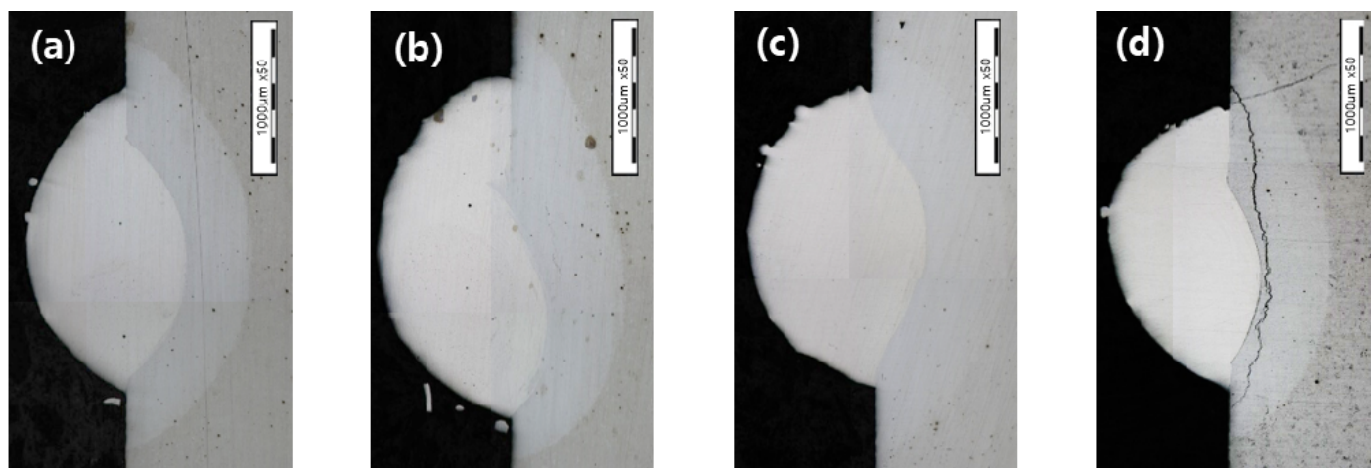


Fig. 3. Cross-sectional shape of rotating direct-metal deposition by combination of 4 pictures, (a) Standard condition, (b) High laser power, (c) Low laser scanning velocity, (d) High powder feed (Table 2 shows the experimental conditions corresponding to each number)

feeding condition (d) forms deposits with cracks because of insufficient fusion; the large amount of powder interferes with the laser path, so the deposition is insufficiently fused.

Fig. 4 shows the microstructural images of asymmetric dilution from Fig. 3(2). The microstructure contains a small amount of pores and is composed of dendrites and inter-dendrites. Differences in size are observed clearly in the low (a-1) and high (b-1) dilution areas because of asymmetric dilution. The microstructures of region (a-2) are small and uniformly distributed, but those in region (b-2) are long with radial orientation to the substrate and non-homogeneous size. In area (b), the substrate is significantly melted and grains grow because of the high laser energy input and low cooling rate thereafter. At low dilution, the dendrites are small at $3.88 \mu\text{m}$ in width and $12.65 \mu\text{m}$ in length;

at high dilution, they are large and long at $5.42 \mu\text{m}$ in width and $24.55 \mu\text{m}$ in length.

Table 3 shows the metallurgical composition according to dilution from Fig. 4. The microstructure contains dendrites of fcc Co-rich solid solution and inter-dendrite spaces of Co-rich and Cr and W carbide phases with a lamellar mixture, formed by eutectic reaction [3]. In the region with high dilution (b), the high laser energy input causes Cr and Co to diffuse from the dendrites to inter-dendrite spaces. Therefore, the intermetallic phase becomes coarsened and the content of very hard carbides is increased [4,5]. Fig. 5 shows the metallurgical composition of the bonding zone from Fig. 4. Fe only penetrates from the substrate to the deposit. This deteriorates the toughness of the coating and thus degrades the properties of the deposited metal [1].

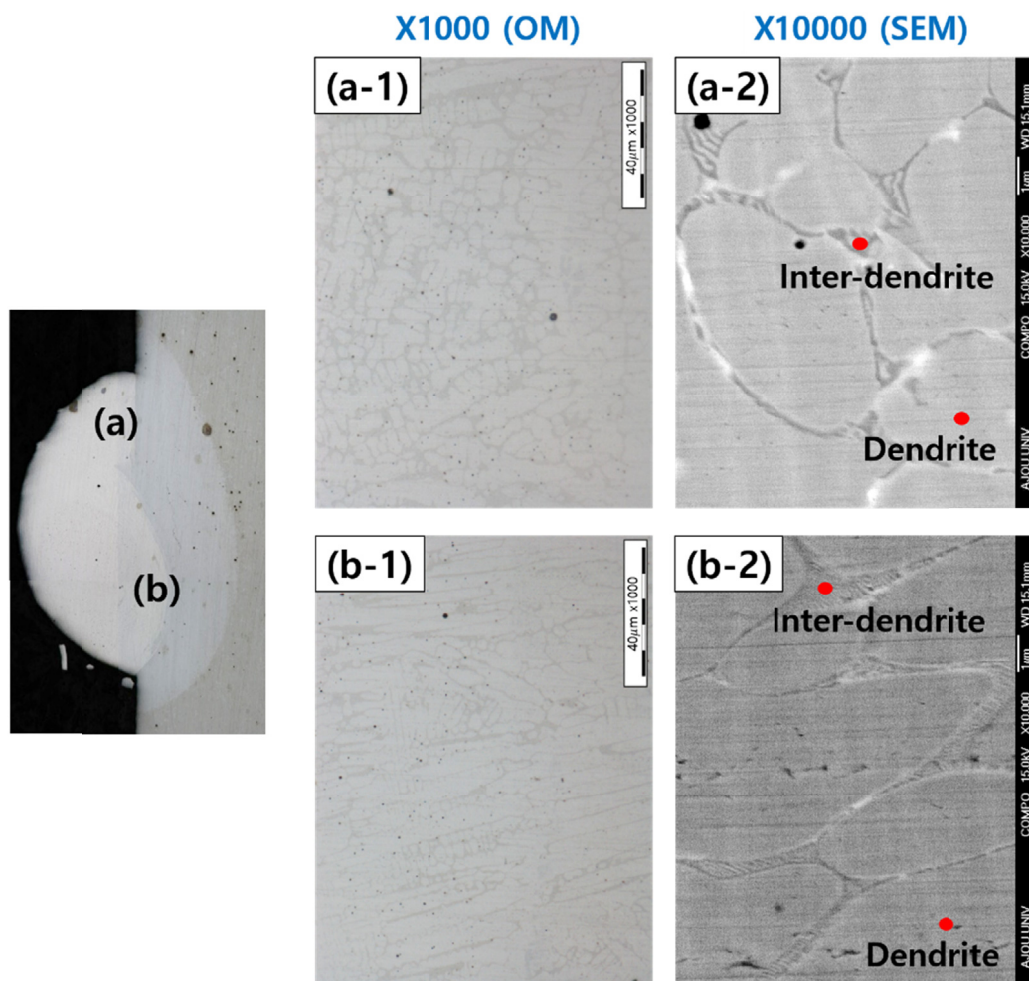


Fig. 4. Microstructure of asymmetric dilution (from the Fig. 3 (2)): (a) low dilution, (a-1) and (a-2) microstructure of (a) location, (b) high dilution, (b-1) and (b-2) micro structure of (b) location

TABLE 3

Metallurgical composition of dendrite and inter-dendrite space by EDS point analysis from the SEM image in Fig. 4 (%)

		C	Cr	Mn	Fe	Co	Mo	W	Si	Total
(a) Low dilution	Inter	5.54	30.90	0.91	24.58	30.01	0.74	7.32	—	100
	Dendrite	2.40	16.72	0.75	35.87	40.31	—	3.12	0.83	100
(b) High dilution	Inter	5.74	32.30	0.98	25.85	26.83	0.74	7.55	—	100
	Dendrite	2.48	17.08	0.76	35.84	42.53	—	—	1.31	100

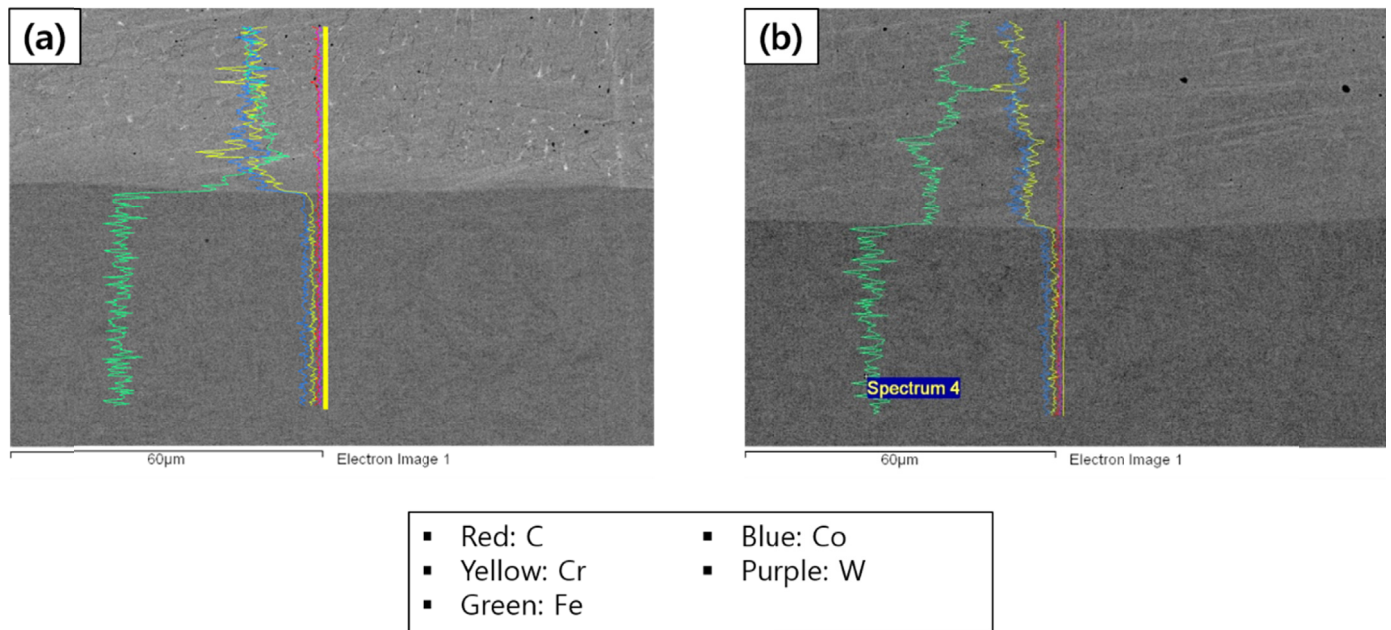


Fig. 5. Metallurgical composition of bonding zone by the EDS line analysis (from the Fig. 4 (a) and (b)): (a) low dilution and (b) high dilution

4. Conclusions

In this study, material analysis of the novel rotating direct-metal deposition method, which can do preliminary surface treatment and damage repair to cylinder inner walls, was performed. At 1.4 kW power, 4 mm/s scanning velocity, and 12 g/min feed rate, an excellent and large-coverage cross-section was obtained without defects and asymmetric dilution. The microstructure of asymmetric dilution showed longer and larger grain sizes than that of the low dilution and was distributed in a radial form in the direction of the substrate. The bulk diffusion of hard carbides from the dendrites to inter-dendrite spaces was increased by high dilution. However, the toughness was lowered because Fe penetrated from the substrate to the deposited layer. In order to obtain a uniform microstructure without asymmetric dilution, the laser energy input should be increased by decreasing the laser scanning velocity.

Acknowledgments

This work was supported by the Energy Efficiency of the Korea Institute of Energy Technology Evaluation and Planning (KETEP) grant funded by the Korea government Ministry of Knowledge Economy and Ministry of Trade, Industry & Energy (MOTIE) (No. 20165010300800).

REFERENCES

- [1] G. Xu, M. Kutsuna, Z. Liu, K. Yamada, *Surf. & Coat. Tech.* **201**, 1138-1144 (2006).
- [2] Deloro, "Stellite 6 Alloy Technical Data," www.stellite.com.
- [3] M.A. Montealegre, A.T. Perez, J.L. Arias, P. Rey, G. Castro, M. Gonzalez, *ResearchGate* **805**, 298-303 (2010).
- [4] A.S. Oliveira, P.S. Silva, R.M.C. Vilar, *Surf. & Coat. Tech.* **153**, 203-209 (2002).
- [5] G.S. Ham, C.O. Kim, S.H. Park, K.A. Lee, *J. of Korean Powder Metall. Inst.* **24** (5), 370-376 (2017).